Phytochemistry 96 (2013) 265–272

Contents lists available at ScienceDirect

Phytochemistry

journal homepage: www.elsevier.com/locate/phytochem

Cytotoxicity of naturally occurring rhamnofolane diterpenes from *Jatropha curcas*

Jie-Qing Liu [1], Yuan-Feng Yang [1], Xu-Yang Li, En-Qian Liu, Zhong-Rong Li, Lin Zhou, Yan Li, Ming-Hua Qiu *

State Key Laboratory of Photochemistry and Plant Resources in West China, Kunming Institute of Botany, Chinese Academy of Sciences, Kunming 650201, Yunnan, PR China

ARTICLE INFO

Article history:
Received 9 March 2013
Received in revised form 14 August 2013
Available online 27 September 2013

Keywords:
Jatropha curcas
Euphorbiaceae
Rhamnofolane diterpenoids
Cytotoxicity

ABSTRACT

Twelve rhamnofolane diterpenoids, including curcusecons A–E with unusual *seco*-rhamnofolane skeletons, curcusones F–J, 4-*epi*-curcusone E, and 3-dehydroxy-2-*epi*-caniojane, together with seven known analogues, curcusones A–E, jatrogrossidione, and 2-*epi*-jatrogrossidione, were isolated from the roots of *Jatropha curcas*. Their structures were determined by extensive spectroscopic methods, and the relative stereochemistry of curcusecon B was further confirmed by X-ray crystallographic data. Their cytotoxity against five human cancer cells was studied and the results indicated that the dienone system in ring B was essential for cytotoxicity of these compounds.

1. Introduction

Jatropha curcas L. (Euphorbiaceae) is attracting much attention for its possible utilization as a biofuel feedstock, as well as its medicinal values. Its seeds contain up to 43–61% oil (Achten et al., 2010; Fairless, 2007) that can be processed to produce a high-quality biodiesel fuel, usable in a standard diesel engine. Meanwhile, the roots of *J. curcas* can be used for the treatment of many diseases including gum bleeding, toothache, eczema, ringworm, scabies, dysentery and gonorrhea (Burkill, 1994; Oliver-Bever, 1986). Previous chemical investigations of *J. curcas* resulted in the identification of diverse types of diterpenes, which can be classified into rhamnofolane, daphnane, lathyrane, tigliane, dinorditerpene, deoxy preussomerin and pimarane according to their skeletal types (Devappa et al., 2011). In addition, some diterpenes with unprecedented skeletons were also reported, such as spirocurcasone (possessing a "spirorhamnofolane" skeleton) (Chianese et al., 2011), jatrophalactam (possessing a novel 5/13/3 tricyclic skeleton) (Wang et al., 2009), and jatrophadiketone (possessing a 6/6/6 tricyclic skeleton) (Liu et al., 2012). Some of the diterpenoids from this species display significant diverse biological activities, exhibiting anti-inflammatory (Pertino et al., 2007), anti-proliferative (Chianese et al., 2011; Sahidin et al., 2011), anti-bacterial (Ravindranath et al., 2003), anti-microbial (Can-Ake et al., 2004; Ekundayo et al., 2011), anti-plasmodial (Sutthivaiyakit et al., 2009), and especially cytotoxic properties (Aiyelaagbe et al., 2011; Liu et al., 2012; Picha et al., 1996; Xu et al., 2011; Zhang et al., 2012).

Curcusones A–D from *J. curcas* are rhamnofolane derivatives (Naengchomnong et al., 1986) reported with significant cytotoxic activity (Aiyelaagbe et al., 2011; Picha et al., 1996). In particular, curcusone B, the content of which being as high as 0.13% in roots of *J. curcas* (Picha et al., 1996), could effectively suppress the metastatic processes at non-cytotoxic doses and showed an anti-invasive effect against cholangiocarcinoma cells (Muangman et al., 2005). Moreover, it also displayed a significant dose-dependent inhibition of cell proliferation of K562 and H1299 cell lines with an IC_{50} of 6 μg/mL and 15.0 μg/mL, respectively (Wang et al., 2009). To the best of our knowledge, despite a number of studies on the anticancer activity of rhamnofolane derivatives, there has been no report on the structure–activity relationships of these diterpenoids.

Motivated by the significant anticancer activity of rhamnofolane derivatives, the chemical constituents of the roots of *J. curcas* collected from Xishuangbanna, Yunnan Province were systematically studied. Twelve new rhamnofolane diterpenes, curcusecons A–E (**1**–**5**), curcusones F–J (**6**–**10**), 4-*epi*-curcusone E (**11**), and 3-dehydroxy-2-*epi*-caniojane (**12**), along with seven known compounds, curcusones A–E (**13**–**17**), jatrogrossidione (**18**), and 2-*epi*-jatrogrossidione (**19**) were isolated (Fig. 1). These nineteen compounds were evaluated for their cytotoxicity against A-549, HL-60, MCF-7, SMMC-7721, and SW480 human cancer cells. Herein, reported are the isolation, structural elucidation, and the anticancer activity of **1**–**19**, as well as structure–activity relationships of these curcusone analogues.

* Corresponding author. Tel.: +86 871 65223327; fax: +86 871 65223255.
E-mail address: mhchiu@mail.kib.ac.cn (M.-H. Qiu).
[1] These authors contributed equally to this work.

0031-9422/$ - see front matter © 2013 Elsevier Ltd. All rights reserved.
http://dx.doi.org/10.1016/j.phytochem.2013.09.008

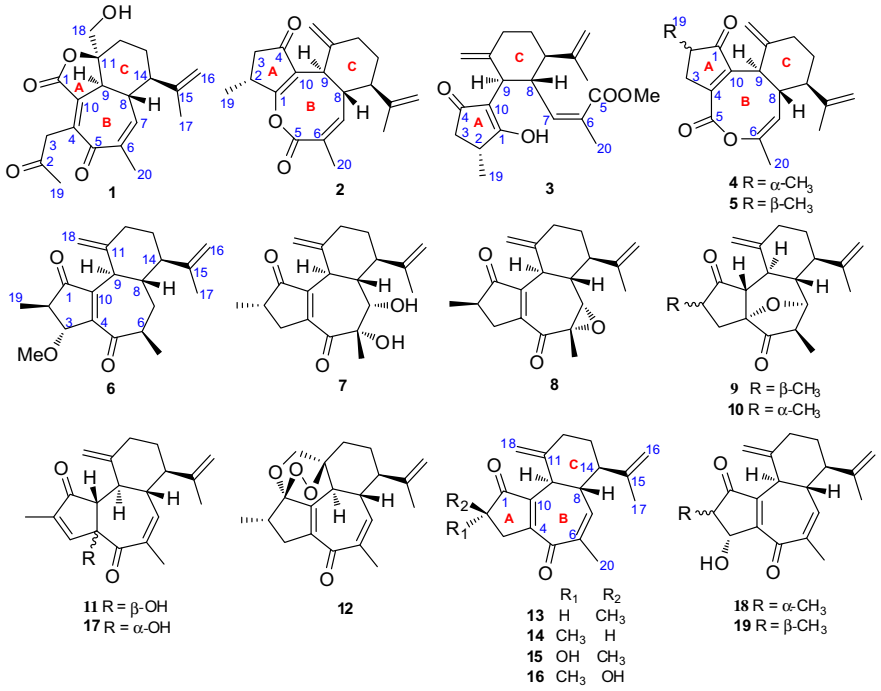

Fig. 1. The structures of **1**–**19**.

2. Results and discussion

Curcusecon A **(1)**, obtained as an amorphous powder, has the molecular formula of $C_{20}H_{24}O_5$ as determined by HREIMS at *m/z* 344.1622 $[M]^+$ (calcd 344.1624), corresponding to 9 degrees of unsaturation. Its IR spectrum showed absorptions for hydroxyl group (3431 cm^{-1}), carbonyl groups (1743 and 1722 cm^{-1}), and an olefinic functionality (1628 cm^{-1}). The UV absorbance at λ_{max} 242 nm indicated the presence of an α,β-unsaturated carbonyl group. The ^{1}H-NMR spectroscopic data (Table 1) indicated the presence of three methyl groups, an olefinic proton, together with an exocyclic methylene group. The ^{13}C-DEPT data (Table 2) of **1** showed 20 carbon signals, including three methyls, five methylenes (one olefinic and one oxygenated), four methines (one olefinic), and eight quaternary carbons (four olefinics, three carbonyls, and one oxygenated). Since its NMR spectroscopic data were similar to those of curcusones A and B (**13** and **14**) (Naengchomnong et al., 1986), compound **1** was deduced to be a rhamnofolane diterpenoid.

The partial structure of **1**, as drawn in blue bold lines in Fig. 2, was established based on its ^{1}H–^{1}H COSY correlations of H_2-12/H_2-13/H-14/H-8/H-7 and of H-8/H-9, as well as the HMBC correlations from the exocyclic methylene protons to C-14, C-15, and C-17; from H_3-20 to C-5, C-6, and C-7; from H-9 to C-4, C-8, C-10,

Table 1
^{1}H NMR spectroscopic data of compounds **1**–**6**.

No.	1[a]	2[a]	3[b]	4[a]	5[a]	6[a]
2		3.09, m	2.40, m	2.45, m	2.63, m	2.86, m
3a/α	4.26, d (17.3)	2.84, dd (18.7, 6.9)	2.55, dd (17.1, 6.9)	2.85, ddd (18.3, 6.8, 2.4)	3.38, ddd (18.1, 7.1, 0.5)	–
3b/β	4.03, d (17.3)	2.14, dd (18.7, 1.9)	1.90, dd (17.1, 1.9)	2.66, dd (17.8, 1.5)	2.27, m	3.39, s
6						2.49, overlapped
7α	6.54, dp (2.5, 1.3)	5.58, dp (9.6, 1.5)	5.47, d (10.5)	4.74, d (9.8)	4.84, dp (9.8, 0.9)	2.81, ddd (18.3, 6.8, 3.0)
7β						2.60, dt (18.3, 2.1)
8	2.43, m	2.60 (td, 11.8, 10.2)	3.51, d (9.9)	2.88, d (11.9)	2.97, d (11.9)	1.67, m
9	3.09, d (11.6)	2.93, d (12.3)	2.92, d (9.9)	2.36, overlapped	2.45, overlapped	1.62, m
12α	2.02, dt (15.6, 5.1)	2.45, ddd (13.3, 4.1, 2.6)	2.47, dt (13.4, 3.2)	2.37, overlapped	2.43, overlapped	2.39, ddd (12.7, 4.5, 2.4)
12β	1.66, overlapped	2.24, m	2.18, dt (13.2, 4.3)	2.18, m	2.26, m	2.30, dt (13.0, 4.6)
13α	1.66, overlapped	1.81, m	1.68, d (3.2)	1.74, m	1.83, m	1.87, m
13β	1.50, m	1.46, dd (13.2, 4.3)	1.64, m	1.41, dd (13.1, 4.2)	1.50, dd (12.6, 4.3)	1.49, m
14	1.92, m	2.21, m	2.11, dt (11.2, 3.8)	2.18, m	2.23, m	2.49, overlapped
16a	4.88, m	4.72, s	4.87, s	4.60, s	4.74, s	4.87, s
16b	4.79, s	4.73, s	4.79, s	4.64, s	4.75, s	4.88, s
17	1.60, s	1.55, s	1.66, s	1.51, s	1.60, s	1.62, s
18a	3.54, d (11.7)	4.74, s	4.66, s	4.12, s	4.25, s	4.67, s
18b	3.47, d (11.7)	4.31, s	4.57, s	4.64, s	4.73, s	4.06, s
19	2.17, s	1.16, d (7.1)	1.10, d (7.2)	1.20, d (7.5)	1.24, d (7.3)	1.16, d (5.8)
20	1.83, brs	1.89, d (1.4)	1.71, s	1.77, s	1.87, s	1.22, d (7.6)
-OMe			3.48, s			3.31 (s)

[a] Recorded in $CDCl_3$.
[b] Recorded in Methanol-d_4. Chemical shift values δ are in ppm and the coupling constant *J* is in Hz (in parentheses).

Table 2
^{13}C NMR spectroscopic data of compounds **1**–**12**.

No.	**1**[a]	**2**[a]	**3**[b]	**4**[a]	**5**[a]	**6**[a]	**7**[a]	**8**[a]	**9**[a]	**10**[a]	**11**[a]	**12**[a]
1	169.1	180.6	207.0	210.3	209.9	204.7	209.9	210.9	210.3	211.9	203.3	108.6
2	205.2	35.0	38.8	39.3	40.2	49.2	40.7	40.3	40.4	42.2	144.8	38.6
3	42.5	42.3	41.6	38.1	38.4	80.3	34.0	36.0	33.0	31.4	152.6	37.3
4	142.6	205.1	200.3	142.7	143.1	160.0	167.9	153.8	84.1	86.6	86.3	136.1
5	193.6	167.2	170.9	167.5	167.5	209.6	207.7	204.5	217.6	215.4	208.0	190.3
6	137.0	126.2	127.4	147.7	147.6	37.3	81.9	64.2	42.1	42.1	136.3	138.1
7	145.0	138.1	147.5	118.0	118.1	33.8	70.2	65.5	82.1	80.4	134.4	140.0
8	40.9	45.4	44.9	46.3	46.5	45.0	47.1	41.2	47.2	41.6	45.5	37.2
9	46.9	43.3	43.9	41.7	41.6	40.6	39.0	43.5	39.5	39.2	43.8	43.6
10	137.5	129.4	114.2	153.6	152.8	142.7	140.5	147.6	55.5	51.9	59.1	149.5
11	83.3	145.6	146.6	146.8	146.7	147.7	146.8	149.5	146.3	142.8	146.7	75.6
12	28.3	35.3	36.8	35.5	35.5	34.2	36.3	36.7	35.3	35.2	36.4	25.6
13	25.9	32.9	32.7	33.2	33.1	32.3	34.0	35.6	33.3	33.5	33.7	28.7
14	46.4	51.8	54.5	51.4	51.4	48.4	47.5	51.9	47.9	48.1	51.9	48.8
15	145.6	146.7	150.4	147.1	147.1	145.4	146.7	146.6	146.0	146.4	150.1	146.0
16	114.6	112.4	111.1	112.0	112.0	111.7	112.9	114.3	112.5	112.4	112.5	113.9
17	18.8	18. 6	19.6	18.5	18.5	17.6	19.1	19.6	18.2	18.5	18.7	18.9
18	69.4	108.1	108.6	107.9	108.1	104.7	106.8	108.4	106.5	109.0	107.0	73.3
19	30.2	17.8	19.0	17.3	15.7	12.9	18.2	14.8	14.5	18.0	10.6	11.0
20	21.5	18.9	21.5	19.8	19.7	15.5	26.8	17.3	15.2	15.6	19.0	20.8
-OMe						55.9						

[a] Recorded in $CDCl_3$.
[b] Recorded in Methanol-d_4.

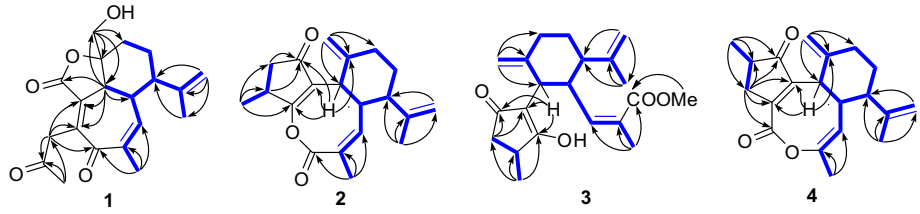

Fig. 2. The ^{1}H–^{1}H COSY (▬), and key HMBC correlations (H → C) of **1**–**4**.

and C-18 (Fig. 2). The oxygenated methylene proton signals of H_2-18 showed cross-peaks to C-9, C-11, and C-12 in its HMBC spectrum, indicating that Me-18 in the curcusone precursor was converted into a CH_2-OH group in **1**.

In the ^{13}C NMR spectrum of **1**, the presence of a lactone carbonyl signal (δ_C 169.2) suggested the cleavage of ring A in the curcusone precursor. In addition, the downfield shift of H_3-19 (δ_H 2.17) in the ^{1}H NMR spectrum and the correlations from H_3-19 to C-2 and C-3, and from H_2-3 to C-2, C-4, C-5, and C-10 in the HMBC spectrum indicated an oxidative C1–C2 cleavage, suggesting a ketone group at C-2. From its ^{1}H and ^{13}C-NMR spectra, it was evident that six degrees of unsaturation were occupied by three carbonyl groups and three pairs of double bonds. Therefore, the molecule should be tricyclic. In addition to rings B and C, the remaining ring was deduced to be a 1,11-γ-lactone by the HMBC correlations from H-9 to C-1, C-10, C-11, and C-18.

The relative stereochemistry of all chiral centers of **1** was assigned through analysis of its ROESY spectrum. NOE correlations of H-9/H-14, H-8/H_3-17 suggested that the stereogenic centers at C-8, C-9, and C-14 have the same relative configurations as those carbons in curcusone B (**14**). The α-orientation of the C-18 hydroxymethyl group was deduced from the ROESY correlation of H-14/H_2-18. Consequently, the structure of **1** was elucidated as an unusual 1,2-*seco*-1,11-γ-lactone rhamnofolane diterpenoid, named curcusecon A.

Curcusecon B (**2**) was obtained as a white powder. Its molecular formula $C_{20}H_{24}O_3$ (nine degrees of unsaturation) was determined on the basis of its HRESIMS data at *m/z* 335.1626 $[M+Na]^+$ (calcd 335.1623). Detailed comparison of the ^{1}H and ^{13}C NMR spectroscopic data (Tables 1 and 2) of **2** with those of curcusone B (**14**) (Naengchomnong et al., 1986) indicated that they were extremely similar and shared the same ring C fragment.

A carbon resonance at δ_C167.2 in its ^{13}C NMR spectrum was ascribed to a lactone carbonyl group, and HMBC correlations from H_3-20 to the lactone carbonyl carbon, an sp^2 quaternary carbon (δ_C 126.2, C-6), and an sp^2 methine (δ_C 138.1, C-7), indicated that the lactone carbonyl was attached to C-5. Furthermore, the IR carbonyl band at 1766 cm^{-1} suggested the presence of a lactone between C-1 and C-5. In addition, HMBC correlations from H_2-3 and H-2 to a ketone carbon (δ_C 205.1) as well as correlations from H-9 to the ketone carbon and a double bond (involving an oxygenated sp^2 quaternary carbon) indicated that the ketonic carbonyl group and the oxygenated sp^2 quaternary carbon were located at C-4 and C-1, respectively. The relative stereochemistry of **2**, as shown in Fig. 3, was finally determined by single-crystal X-ray diffraction analysis.

Curcusecon C (**3**) had a molecular formula of $C_{21}H_{28}O_3$, as deduced by its HREIMS $[M]^+$ 344.1997 (calcd 344.1988) data, possessing eight degrees of unsaturation (one less than that of **2**). The ^{1}H-NMR spectrum of **3** (Table 1) was very similar to that of **2**, except for an additional methoxyl signal at δ_H 3.48 (s) in **3**. Their ^{13}C-NMR spectroscopic data (Table 2) suggested that these two compounds shared the same A and C rings. Nevertheless, the carbon signal of C-1 in **3** was strikingly deshielded relative to that of in **2**, indicating that the eight-membered 1,5-lactone in **2** was opened in **3**. This assumption was in accordance with the degrees of unsaturation of **3**. The HMBC correlations from H_3-19 to C-1, C-2, and an oxygenated sp^2 quaternary carbon (δ_C 206.0) confirmed the

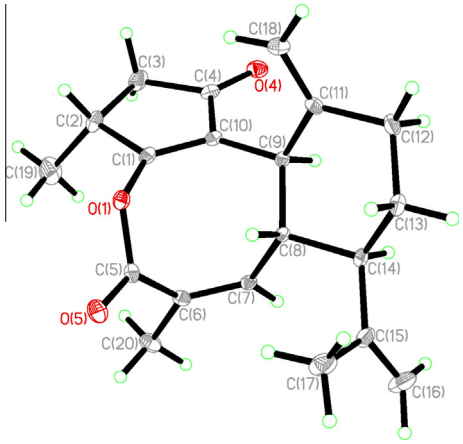

Fig. 3. X-ray crystal structure of compound **2**.

location of a hydroxyl group at C-1. The methoxy group attached to C-5 was deduced by HMBC correlation from the OMe proton (δ_H 3.48, s) to C-5 (δ_C 170.9). The Δ^6 double bond was assigned as *Z* configuration by the ROESY correlation of H-7 with Me-20. Finally, the structure of **3** was characterized and named curcusecon C.

Compound **4** had the same molecular formula $C_{20}H_{24}O_3$ as **2**, established by the HRESIMS at *m/z* 335.1630 $[M+Na]^+$ (calcd 335.1623). The MS and 1D-NMR spectroscopic data of **4** indicated that it was also a tricyclic diterpene lactone. However, the characteristic resonance at δ_C 180.6 (C-1) in **2** was absent and replaced by the downfield resonance at δ_C 210.3 in **4**. Comparison of the ^{13}C-NMR spectroscopic data of **2** and **4** established that the signal of C-6 at δ_C 126.2 in **2** shifted downfield to δ_C 147.7 in **4**, while the resonance of C-7 at δ_C 138.1 in **2** was shifted upfield to δ_C 118.0 in **4**. These data suggested that **4** was a 5,6-*seco*-curcusone lactone. The proposed structure was further supported by the facts that the proton signal H_3-20 displayed no correlation with the ester carbonyl carbon but was instead correlated with C-6 and C-7 in the HMBC spectrum of **4** (Fig. 2).

Compound **5** was found by HRESIMS to have the same molecular formula $C_{20}H_{24}O_3$ as **4**. Detailed comparison of the 1D-NMR spectroscopic data of **5** with those of **4** made it clear that **4** and **5** possessed the same gross structure, and the only difference was the chemical shift of C-19, which suggested that they might be C-2 epimers. The difference in the chemical shift of C-19 was then exploited to place the orientation of Me-19. In comparison with literature data (Naengchomnong et al., 1986) as well as that of **2** (17.8 ppm), compound **4** (17.3 ppm) was assigned to have an alpha-19-Me while compound **5** (15.7 ppm) a beta-19-Me. Compounds **4** and **5** were named curcusecons D and E, respectively.

Curcusone F (**6**) was isolated as white powder. Its molecular formula was determined to be $C_{21}H_{28}O_3$ by HREIMS (*m/z* for $[M]^+$; found 328.2043, calcd 328.2038) data. ^{1}H-NMR spectrum displayed characteristic resonances for four methyls (including one methoxy), one oxygenated methine at δ_H 3.39 (br s, H-3), and two olefinic methylenes at δ_H 4.88, 4.87, 4.67, and 4.06. Comparison of the 1D-NMR spectroscopic data of **6** (Tables 1 and 2) with those of 2-*epi*-jatrogrossidione (**18**) (Jakupovic et al., 1988) indicated that many structural similarities except for a reduction of the Δ^6 double bond and a replacement of the 3-OH by a methoxyl group (Fig. 4). Firstly, the reduction of Δ^6 double bond clearly leads to a methylene and a methine, which was proved by the HMBC (Fig. 4) correlations of H_3-20 with C-5, C-6, and C-7, in combination with the correlations of H-6/H-7/H-8 in the ^{1}H–^{1}H COSY spectrum. Secondly, the 3-OH in **18** was replaced by a 3-OMe group in **6**, which was supported by HMBC correlations from the OMe proton (δ_H 3.31) to C-3 and from H-3 to C-1, C-2, and C-19.

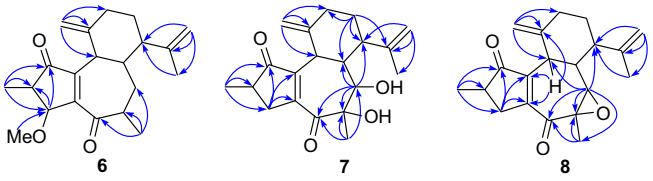

Fig. 4. Key HMBC correlations (H → C) for compounds **6**–**8**.

The configuration of Me-19 was deduced to be β based on the chemical shifts of H_3-19 (δ_H 1.16) and C-19 (δ_C 12.9), which is in good agreement with those in 2-*epi*-jatrogrossidion (Jakupovic et al., 1988). In the ROESY spectrum of **6**, correlation of H-3 with Me-19 suggested that the 3-OMe group was α-oriented. Biogenetically, these types of diterpenoids are derived from lathyrane diterpenes (Sutthivaiyakit et al., 2003); therefore, Me-20 was assigned to be β-oriented. Thus, compound **6** was identified as 2-*epi*-3-methoxy-6,7-dihydrojatrogrossidion.

Curcusone G (**7**) was determined to have the molecular formula of $C_{20}H_{26}O_4$ from HREIMS (*m/z* 330.1823 $[M]^+$; calcd 330.1831) analysis, which was supported by positive ESIMS peaks at *m/z* 353 $[M+Na]^+$ and 683 $[2M+Na]^+$. The HSQC correlations from H_2-3 [δ_H 3.03 (overlapped); 1.89 (overlapped)] and H_2-13 [δ_H 1.54 (m); 1.45 (m)] to the carbon signal at δ_C 34.0 (a methylene signal by the DEPT spectrum) established it represented signals of two overlapping methylenes, which were then assigned to C-3 and C-13 on the basis of HMBC correlations from H_2-3 to Me-19, C-1, C-4, and C-10, and from H_2-13 to C-8, C-11, C-14, and C-15. Twenty skeletal carbon resonances, consisting of three methyls, five methylenes (two terminal double bonds), five methines (one oxygenated), and seven quaternary carbons (two carbonyls and four olefinics), were therefore recognized. These spectroscopic data bore a resemblance to those of curcusone B (**14**), except for the dihydroxylation of Δ^6 double bond, which was confirmed by the HMBC correlations of H-7 with C-5, C-6, C-8, and C-14, and of Me-20 with C-5, C-6, and C-7. ROESY correlations from H-7 and H-8 to Me-20 indicated that the two hydroxyl groups were α-oriented. The ^{13}C-NMR chemical shift of Me-19 (δ_C 18.2), similar to that of in **14** (δ_C 18.5), suggested that Me-19 in **7** has the same α-orientation as in **14**. Finally, the structure of **7** was assigned to be curcusone G.

The molecular formula of curcusone H (**8**) was found to be $C_{20}H_{24}O_3$ as inferred by HREIMS analysis (*m/z* 312.1718 $[M]^+$; calcd 312.1725), with 9 degrees of unsaturation. Detailed comparison of the ^{1}H- and ^{13}C-NMR spectroscopic data (Tables 2 and 3) with those of curcusone A (**13**) indicated that they were structural analogues, except that the double bond between C-6 and C-7 in **13** was replaced by an epoxide group, as suggested by an oxymethine (δ_C 65.5) and an oxygenated quaternary carbon (δ_C 64.2) in **8**. This evidence was confirmed by the observed HMBC correlations from H-7 to C-5, C-6, C-9, C-14, and C-20. ROESY correlations of H-7 with H-8 and Me-20 indicated that the 6,7-epoxide ring was in α-orientation. The relative configuration of Me-19 was deduced to be the same as that of **13** from their similar ^{1}H- and ^{13}C-NMR spectroscopic data. Thus, the structure of **8** was established and named curcusone H.

Curcusone I (**9**) was isolated as needles. Its HRESIMS (*m/z* 315.1962 $[M+H]^+$; calcd 315.1960) gave a molecular formula at $C_{20}H_{26}O_3$, requiring 8 degrees of unsaturation. From the 1D-NMR spectroscopic data (Table 2), four degrees of unsaturation were ascribed to two C=O groups and two C=C moieties. Thus, the structure of **9** is tetracyclic. Its spectroscopic data were similar to those of curcusone A (**13**), apart from the loss of the two double bonds in ring B and the appearance of a 4,7-cyclic ether. HMBC correlations from H-7 to C-4 (δ_C 84.1), C-5, C-9, and C-20, combined with the

Table 3
^{1}H NMR spectroscopic data of compounds **7**–**12** in $CDCl_3$ (δ in ppm, *J* in Hz).

No.	7	8	9	10	11	12
2	2.48, dd (13.9, 6.5)	2.48, m	2.78, m	2.56, dd (16.2, 8.6)		2.33, dd (15.2, 7.6)
3α	3.03, overlapped	3.25, ddd (18.1, 7.2, 2.4)	2.52, m	1.67, m	6.66 (br s)	2.93, m
3β	1.89, ovelapped	2.13, overlapped	1.82, dd (7.9, 3.4)			
6			2.36, dd (14.8, 7.3)	2.46, m		
7	3.70, s	3.35, s	4.05, d (3.1)	4.02, d (2.3)	5.51, dd (7.1, 1.6)	6.28, dd (3.6, 1.4)
8	1.80, m	2.11, overlapped	1.79, dd (5.8, 3.4)	1.96, dd (13.3, 4.0)	2.02 ,dt (11.4, 7.5)	2.27, m
9	3.03, overlapped	3.12, d (11.2)	2.08, m	2.28, dd (12.4, 3.4)	3.19, d (11.8)	2.74, m
10			2.92, dd (11.2, 2.3)	2.86, d (4.7)	3.32, s	
12α	2.44, m	2.41, m	2.41, m	2.46, m	2.44, m	1.54, m
12β	2.30, m	2.29, m	2.14, m	2.08, m	2.25 ,dt (13.1, 4.5)	
13α	1.89, ovelapped	1.95, m	1.76, m	2.15, dd (13.6, 8.6)	1.82, m	1.84, m
13β	1.54, m	1.42, m	1.55, m	1.94, m	1.42, ddd (25.6, 13.1, 4.4)	1.45, m
14	2.56, dt (11.8, 3.9)	2.56, m	2.06, m	1.90, dd (11.5, 3.5)	2.34, dt (11.7, 3.7)	2.01, m
16a	4.83, s	4.92, s	4.77, s	4.79, s	4.72, s	4.88, s
16b	4.83, s	4.93, s	4.72, s	4.73, s	4.73, s	4.82, s
17	1.67, s	1.67, s	1.67, s	1.68, s	1.51, s	1.61, s
18a	4.82, s	4.90, s	4.81, s	4.92, s	5.06, s	4.26, d (9.6)
18b	4.34, s	4.05, s	4.44, s	4.72, s	4.83, s	3.88, d (9.6)
19	1.24, d (7.7)	1.22, d (7.2)	1.26, d (7.2)	1.28, d (5.8)	1.90, d (1.5)	1.06, d (7.3)
20	2.34, s	1.50, s	1.21, d (7.5)	1.26, d (5.8)	1.62, s	1.87, s
4-OH					4.26, s	

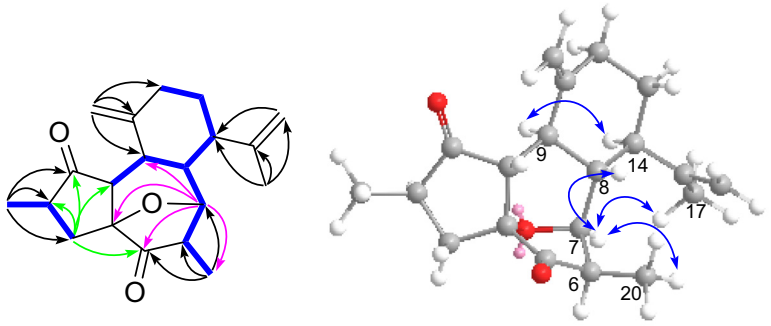

Fig. 5. The ^{1}H–^{1}H COSY (—), key HMBC correlations (H → C), and key ROESY correlations (↷) of compound **9**.

^{1}H–^{1}H COSY correlations of H-10/H-9 and of H-8/H-7, supported the presence of the 4,7-oxygen bridge. In the ROESY spectrum of **9** (Fig. 5), NOE correlations between: H-7 with H_3-20, H_3-17, and H-8; H-10 with H-8; and H-9 with H-14 suggested that H-7, H-8, H-10, and H_3-20 were all β-oriented while H-9 and H-14 were α-oriented. The chemical shift of C-19 (δ_C 14.5) suggested a β configuration of Me-19 (Naengchomnong et al., 1986). Therefore, a structure **9** was identified and named as curcusone I.

Curcusone J (**10**) had the same molecular formula, $C_{20}H_{26}O_3$, as compound **9** in the light of the HRESIMS (*m/z* 315.1966 $[M+H]^+$; calcd 315.1960). Comparison of the spectroscopic data of **9** and **10** indicated that they were C-2 epimers. The observation of ROESY correlations from H-7 to H_3-20, H_3-17, and H-8 indicated that the 4,7-oxygen bridge in **10** had the same orientation as in **9**.

The molecular formula and the spectroscopic data of compound **11**, 4-*epi*-curcusone E, indicated that it was isomeric with curcusone E (**17**) (Chianese et al., 2011). A minor difference was the carbon signal for C-4 shifted upfield (δ_C 86.3) in **11** relative to that of (δ_C 88.9) in curcusone E. The overall structure of **11** was deduced from its COSY and HMBC spectra (Fig. 6). The ROESY correlations of 4-OH/H-10, 4-OH/H-8, and H-10/H-18a confirmed the structure and showed that both 4-OH and H-10 were β-oriented.

3-Dehydroxy-2-*epi*-caniojane (**12**), which crystallized as needles (MeOH), had a molecular formula of $C_{20}H_{24}O_4$ by HRESIMS (*m/z* 329.1744 $[M+H]^+$; calcd 329.1752). The IR spectrum showed absorptions for unsaturated carbonyl (1680 cm^{-1}) and olefinic (1608 cm^{-1}) groups. The ^{1}H-NMR and ^{13}C-DEPT data (Tables 2 and 3) of **12** were closely related to those of 2-*epi*-caniojane (Sutthivaiyakit et al., 2003). However, a methylene at C-3 (δ_C 37.3) in **12** replaced an oxymethine (δ_C 74.9) in 2-*epi*-caniojane as indicated by the HMBC correlations from H_3-19 (δ_H 1.06, d, *J* = 7.3 Hz) to C-1, C-2, and C-3 (δ_C 37.3), and from H_2-3 to C-1, C-4, C-5, and C-10. The β-orientation of Me-19 was established by comparison of the chemical shifts, splitting patterns, and coupling constants of H_3-19 (δ_H 1.06, d, *J* = 7.3 Hz) of **12** with those of literature values (H_3-19: δ_H 1.01, d, *J* = 7.6 Hz) reported for 2-*epi*-caniojane (Sutthivaiyakit et al., 2003). The stereochemistry of the peroxy bond between C-1 and C-11 were assigned as β-oriented based on the cross-peaks between H_2-18 and H-9 in the ROESY spectrum.

The structures of known compounds, curcusones A–E (**13**–**17**) (Chianese et al., 2011; Naengchomnong et al., 1986), jatrogrossidione (**18**) (Jakupovic et al., 1988), and 2-*epi*-jatrogrossidione (**19**) (Jakupovic et al., 1988), were elucidated by comparison of their spectroscopic date with those reported.

All the naturally occurring rhamnofolane diterpenoids **1**–**19** were evaluated for their cytotoxicity against five the tumor cell lines including HL-60 (leukemia), SMMC-7721 (hepatoma), A-549 (lung cancer), MCF-7 (breast cancer), and SW480 (colon cancer) using the MTT assay, with cisplatin as the positive control. The results are summarized in Table 4. Curcusones A–D (**13**–**16**), as abundant constituents in the roots of *J. curcas*, showed remarkable inhibitory effects against the above cell lines with the IC_{50} values ranging from 1.36 to 4.70 μM. 3-Dehydroxy-2-*epi*-caniojane (**12**)

Table 4
Cytotoxicity data of compounds **1**–**19** with IC_{50} values (μM).

No.	HL-60	SMMC-7721	A-549	MCF-7	SW480
1–11	>40	>40	>40	>40	>40
12	2.86	3.94	3.94	11.69	14.05
13	1.63	3.10	3.35	2.47	2.10
14	2.64	3.30	3.88	3.14	2.91
15	1.36	2.17	3.88	1.61	1.99
16	2.81	3.58	4.70	2.77	2.83
17	>40	>40	>40	>40	>40
18	22.80	19.49	34.93	21.83	20.06
19	23.30	18.36	36.53	22.72	21.08
Cisplatin	1.14	14.51	12.76	19.61	17.54

exhibited IC_{50} values of 2.86, 3.94, 3.94, 11.69, and 14.05 μM against the above cells, respectively. The structure–activity relationship analysis indicates that the basic structural requirement for the cytotoxic activity of the curcusone analogues is the ring B dienone system. Thus, hydrogenation and/or oxidation of the conjugated C4/10 or C6/7 double bonds, as in **6**–**11** and **17**, led to essentially inactive compounds. Also, when the conjugated C-5 ketone group was converted into an ester or a lactone group, as in **2**–**5**, they displayed no cytotoxicity. It seems that once the ring B dienone system is disrupted, the cytotoxicity of these compounds decreases significantly. A comparison of the cytotoxic activity of curcusones A–D (**13**–**16**) established that the relative configuration of Me-19 and the addition of a hydroxyl at C-2 did not affect their cytotoxicity. Compounds **18** and **19** were significantly less active than **13** and **14**, indicating that the hydroxyl group at C-3 could reduce the anticancer potency of curcusone derivatives. Further investigations of the anticancer potential and the mechanism(s) of action of these rhamnofolane diterpenoids are in progress and will be reported in due course.

3. Conclusion

A phytochemical investigation of the roots of *J. curcas* resulted in the isolation and characterization of 12 new (**1**–**12**) and seven known (**13**–**19**) rhamnofolane diterpenoids. Of particular interest is the isolation of 1,2-cleaved (curcusecon A), 4,5-cleaved (curcusecons B and C), and 5,6-cleaved (curcusecons D and E) rhamnofolane diterpenoid derivatives. All the isolates have been tested for their cytotoxicity against A-549, HL-60, MCF-7, SMMC-7721, and SW480 human cancer cells. Analysis of the structural features and the activity of these compounds suggested that the dienone system in ring B is an essential requirement for the cytotoxic activity of these rhamnofolane diterpenoids. More in-depth and systematic studies through structural modifications are required in order to reveal details of the structure–activity relationship of these fascinating diterpenes.

4. Experimental

4.1. General experimental procedures

Melting point was determined on X-4 apparatus and was uncorrected. Optical rotations were determined on a JASCO P-1020 digital polarimeter (Horiba, Tokyo, Japan). UV spectra were carried out on a Shimadzu UV-2401PC spectrophotometer (Shimadzu, Kyoto, Japan). IR (KBr) spectra were taken on a Bio-Rad FTS-135 spectrophotometer (Bio-Rad, Hercules, CA, USA). NMR spectra were obtained on a Bruker AVANCE III-600 spectrometer with TMS as the internal standard. Unless otherwise specified, chemical shifts (δ) are expressed in ppm with respect to the solvent signals. ESIMS and HRESIMS were recorded on a VG Auto Spec-3000 mass spectrometer, while HREIMS was measured on an Autospec Premier P776 mass spectrometer. Semi-preparative HPLC was performed on an Agilent 1100 liquid chromatograph with YMC-Pack$ProC_{18}$RS (YMC, 250 × 10 mm, 5 μm) column. Column chromatography (CC) was performed with silica gel (200–300 mesh, Qingdao Marine Chemical Factory, Qingdao, People's Republic of China), Lichroprep RP-18 gel (40–63 μm, Merck, Darmstadt, Germany), or Sephadex LH-20 (General Electric Company, Fairfield, CT); Fractions were monitored by TLC under UV light, and spots were visualized by heating silica gel plates sprayed with 10% H_2SO_4 in EtOH. All solvents including petroleum ether (60–90 °C) were distilled prior to use.

4.2. Plant material

Roots of *J. curcas* were collected in Xishuangbanna, Yunnan Province, People's Republic of China, in September 2010, and were identified by Prof. Chengyuan Yang. A voucher specimen (No. KIB 2010–09-11) has been deposited at the State Key Laboratory of Phytochemistry and Plant Resources in West China, Kunming Institute of Botany, Chinese Academy of Sciences,

4.3. Extraction and isolation

Air-dried roots (5.5 kg) were coarsely powdered and extracted with MeOH (3 × 18 L, each 4 h) at 55 °C. The combined MeOH solution was evaporated in vacuo to afford a crude extract, which was suspended in H_2O and then extracted with $CHCl_3$. The $CHCl_3$ extract (150.0 g) was subjected to silica gel with a Me_2CO/petroleum ether (PE) gradient system (1:15, 1:10, 1:5, 1:2, and 0:1), to yield five main fractions Fr.1–Fr.5. Fraction Fr.1 (Me_2CO/PE, 1:15, v/v; 30.0 g) was applied on an ODS column (450 g, 40–63 μm, 3.5 × 45.0 cm) eluting with MeOH–H_2O (55:45, 65:35, and 80:20, v/v) to give three subfractions Fr.1.1–Fr.1.3. Subfraction Fr.1.1 (5 g) was further fractionated with Fr.1.1.1 was separated by a Sephadex LH-20 column (500.0 g, 2.6 × 95.0 cm; MeOH) to get Fr.1.1.1 (1.7 g) and Fr.1.1.2 (2.8 g), and a semi-preparative reversed-phase HPLC (3 mL/min, UV detection at λmax = 210 nm, CH3OH/H2O, 75:25) to yield two mixtures which were individually purified by silica gel CC (45.0 g, 4.5 × 25.0 cm; PE/$CHCl_3$, 5:1, v/v) to yield **11** (12 mg) and **13** (11 mg). Subfraction Fr.1.2 (15 g) was partitioned by silica gel CC (120.0 g, 4.5 × 25.0 cm; PE/$CHCl_3$, 5:1, v/v) to afford **14** (50 mg) and **15** (45 mg). Subfraction Fr.1.3 (8 g) was further separated by silica gel CC (150.0 g, 3.5 × 40.0 cm; PE/Me_2CO, 15:1, v/v) to give fractions Fr.1.3.1–Fr.1.3.3. Subsequently, fraction Fr.1.3.1 (120 mg) was purified using silica gel CC (15.0 g, 1.8 × 25.0 cm; PE/$CHCl_3$, 5:1, v/v) to give subfractions Fr.1.3.1.1 (28 mg), Fr.1.3.1.2 (55 mg) and Fr.1.3.1.3 (30 mg). Subfraction Fr.1.3.1.1 was decolorized on Sephadex LH-20 with MeOH to give a light brown gum (15 mg). The later was further purified by semi-preparative HPLC (3 mL/min, UV detection at λ_{max} = 210 nm, CH_3OH/H_2O, 80:20) to provide **8** (2.3 mg). Subfraction Fr.1.3.1.2 was further purified by RP-18 CC (CH_3OH/H_2O, 75:25) to afford **2** (12 mg) and with CH_3OH/H_2O, 80:20, to afford an inseparable mixture (35 mg) which was subsequently purified by preparative TLC (PE/$CHCl_3$, 3:1, v/v) to yield **4** (5 mg) and **5** (3 mg), respectively. Subfraction Fr.1.3.1.3 was further purified by semi-preparative HPLC (3 mL/min, UV detection at λ_{max} = 210 nm, CH_3OH/H_2O, 75:25) to yield **12** (8 mg). Subfraction Fr.1.3.2 was purified with semi-preparative HPLC (3 mL/min, UV detection at λ_{max} = 210 nm, CH_3OH/H_2O, 80:20) to give **6** (2.3 mg). Fraction Fr.1.3.3 (45 mg) was purified by a preparative TLC (PE/Me_2CO, 15:1, v/v) to yield **9** (4 mg) and **10** (2 mg). Fraction Fr.2 (Me_2CO/PE, 1:10, v/v; 20.0 g) was subjected to on RP-18 CC with MeOH/H_2O (50:50, 62:38, and 75:25, v/v) to obtain subfraction Fr.2.1–Fr.2.3. Subsequently, subfraction Fr.2.2 (6 g) was separated by silica gel column

(120.0 g, 4.5 × 25.0 cm; $CHCl_3$/Me_2CO, 50:1, v/v) to afford **16** (150 mg), **17** (100 mg), **18** (5 mg), and **19** (6 mg), respectively. Subfraction Fr.2.3 (MeOH/H_2O, 70:30; 6 g) was eluted using silica gel CC (PE/Me_2CO, from 15:1 to 5:1), yielding fractions Fr.2.3.1–Fr.2.3.3. Fraction Fr.2.3.1 and Fr.2.3.2, were, respectively, further purified by semi-preparative reversed-phase HPLC (3 mL/min, UV detection at λ_{max} = 210 nm, CH_3CN/H_2O, 50:50) to yield **3** (4.5 mg) in Fr.2.3.1 and **1** (1.2 mg) in Fr.2.3.2. Fraction Fr.3 (Me_2CO/PE, 1:5, 15 g) was fractionated by repeated CC. First RP-18 CC was used with a gradient elution with MeOH/H_2O (45:55, 55:45, and 70:30, v/v) to yield subfractions Fr.3.1–Fr.3.3. Subsequently, subfraction Fr.3.3 (3 g) was further purified by silica gel CC (PE/Me_2CO, from 10:1 to 5:1) and by semi-preparative reversed-phase HPLC eluted with CH_3CN/H_2O (42:58) to afford **7** (2.3 mg).

4.3.1. Curcusecon A (**1**)

White, amorphous powder; $[\alpha]_D^{25}$ − 86.2 (*c* 0.08, $CHCl_3$); UV/Vis ($CHCl_3$) λ_{max} (log ε) 243 (3.95) nm; IR (KBr) ν_{max} 3439, 2923, 1743, 1722, 1628, 1454 cm^{-1}; ESIMS *m/z* 367 $[M+Na]^+$; HRESIMS *m/z* 344.1622 $[M]^+$ (calcd for $C_{20}H_{24}O_5$ $[M]^+$, 344.1624); For ^1H and ^{13}C NMR spectroscopic data, see Tables 1 and 2.

4.3.2. Curcusecon B (**2**)

Colorless needles; mp 152–155 °C; $[\alpha]_D^{25}$ − 222.4 (*c* 0.10, $CHCl_3$); UV/Vis ($CHCl_3$) λ_{max} (log ε) 241 (3.82) nm; IR (KBr) ν_{max} 2926, 1766, 1698, 1655, 1277, 1168, 1039, 896 cm^{-1}; ESIMS *m/z* 335 $[M+Na]^+$; HRESIMS *m/z* 335.1626 $[M+Na]^+$ (calcd for $C_{20}H_{24}O_3Na$ $[M+Na]^+$, 335.1623); For ^1H and ^{13}C NMR spectroscopic data, see Tables 1 and 2.

4.3.3. Curcusecon C (**3**)

White, amorphous powder; $[\alpha]_D^{25}$ + 13.2 (*c* 0.26, CH_3OH); UV/Vis ($CHCl_3$) λ_{max} (log ε) 269 (4.22), 203 (4.14) nm; IR (KBr) ν_{max} 2933, 1739, 1713, 1648, 1171, 891 cm^{-1}; ESIMS *m/z* 367 $[M+Na]^+$; HREIMS *m/z* 344.1997 $[M]^+$ (calcd for $C_{20}H_{24}O_3$ $[M]^+$, 344.1988); For ^1H and ^{13}C NMR spectroscopic data, see Tables 1 and 2.

4.3.4. Curcusecon D (**4**)

Colorless powder; $[\alpha]_D^{25}$ − 106.4 (*c* 0.10, $CHCl_3$); UV/Vis ($CHCl_3$) λ_{max} (log ε) 241 (3.70) nm; IR (KBr) ν_{max} 2933, 1739, 1713, 1648, 1171, 891 cm^{-1}; ESIMS *m/z* 335 $[M+Na]^+$; HRESIMS *m/z* 335.1630 $[M+Na]^+$ (calcd for $C_{20}H_{24}O_3Na$ $[M+Na]^+$, 335.1623); For ^1H and ^{13}C NMR spectroscopic data, see Tables 1 and 2.

4.3.5. Curcusecon E (**5**)

Colorless powder, $[\alpha]_D^{25}$ − 208.0 (*c* 0.12, $CHCl_3$); UV/Vis ($CHCl_3$) λ_{max} (log ε) 241 (3.79) nm; IR (KBr) ν_{max} 2923, 1730, 1710, 1649, 1169, 895 cm^{-1}; ESIMS *m/z* 335 $[M+Na]^+$; HRESIMS *m/z* 335.1627 $[M+Na]^+$ (calcd for $C_{20}H_{24}O_3Na$ $[M+Na]^+$, 335.1623); For ^1H and ^{13}C NMR spectroscopic data, see Tables 1 and 2.

4.3.6. Curcusone F (**6**)

White, amorphous powder; $[\alpha]_D^{25}$ − 67.2 (*c* 0.23, $CHCl_3$); UV/Vis ($CHCl_3$) λ_{max} (log ε) 249 (4.13) nm; IR (KBr) ν_{max} 3432, 1713, 1648 cm^{-1}; ESIMS *m/z* 351 $[M+Na]^+$; HREIMS *m/z* 328.2043 $[M]^+$ (calcd for $C_{21}H_{28}O_3$ $[M]^+$, 328.2038). For ^1H and ^{13}C NMR spectroscopic data, see Tables 1 and 2.

4.3.7. Curcusone G (**7**)

White, amorphous powder; $[\alpha]$ $[\alpha]_D^{25}$ − 237.9 (*c* 0.22, $CHCl_3$); UV/Vis ($CHCl_3$) λ_{max} (log ε) 241 (4.44), 193 (3.62) nm; IR (KBr) ν_{max} 3440, 2928, 1691, 1639 cm^{-1}; ESIMS *m/z* 353 $[M+Na]^+$; HREIMS *m/z* 330.1823 $[M]^+$ (calcd for $C_{20}H_{26}O_4$ $[M]^+$, 330.1831); For ^1H and ^{13}C NMR spectroscopic data, see Tables 2 and 3.

4.3.8. Curcusone H (**8**)

White, amorphous powder; $[\alpha]_D^{25}$ − 89.8 (*c* 0.18, $CHCl_3$); UV/Vis ($CHCl_3$) λ_{max} (log ε) 257 (4.02) nm; IR (KBr) ν_{max} 3441, 3431, 2927, 1715, 1648 cm^{-1}; ESIMS *m/z* 335 $[M+Na]^+$; HREIMS *m/z* 312.1718 $[M]^+$ (calcd for $C_{20}H_{24}O_3$ $[M]^+$, 312.1725); For ^1H and ^{13}C NMR spectroscopic data, see Tables 2 and 3.

4.3.9. Curcusone I (**9**)

Needle crystals; $[\alpha]_D^{25}$ − 187.6 (*c* 0.17, $CHCl_3$); UV/Vis ($CHCl_3$) λ_{max} (log ε) 274 (2.80), 238 (2.94) nm; IR (KBr) ν_{max} 1728, 1700, 1060 cm^{-1}; ESIMS *m/z* 337 $[M+Na]^+$; HRESIMS *m/z* 315.1962 $[M+H]^+$ (calcd for $C_{20}H_{27}O_4$ $[M+H]^+$, 315.1960); For ^1H and ^{13}C NMR spectroscopic data, see Tables 2 and 3.

4.3.10. Curcusone J (**10**)

White, amorphous powder; $[\alpha]_D^{25}$ − 93.3 (*c* 0.70, $CHCl_3$); UV/Vis ($CHCl_3$) λ_{max} (log ε) 274 (2.50), 238 (2.84) nm; IR (KBr) ν_{max} 1726, 1702, 1058 cm^{-1}; ESIMS *m/z* 337 $[M+Na]^+$; HRESIMS *m/z* 315.1966 $[M+H]^+$ (calcd for $C_{20}H_{27}O_4$ $[M+H]^+$, 315.1960); For ^1H and ^{13}C NMR spectroscopic data, see Tables 2 and 3.

4.3.11. 4-epi-curcusone E (**11**)

Colorless powder, $[\alpha]_D^{25}$ − 86.0 (*c* 0.10, $CHCl_3$); UV/Vis ($CHCl_3$) λ_{max} (log ε) 240 (3.60) nm; IR (KBr) ν_{max} 3435, 2933, 1700, 1678, 1660 cm^{-1}; ESIMS *m/z* 335 $[M+Na]^+$; HRESIMS *m/z* 335.1629 $[M+Na]^+$ (calcd for $C_{20}H_{24}O_3Na$ $[M+Na]^+$, 335.1623); For ^1H and ^{13}C NMR spectroscopic data, see Tables 2 and 3.

4.3.12. 3-Dehydroxy-2-epi-caniojane (**12**)

White, needle crystals; $[\alpha]_D^{25}$ − 288.1 (*c* 0.13, $CHCl_3$); UV/Vis ($CHCl_3$) λ_{max} (log ε) 248 (3.90) nm; IR (KBr) ν_{max} 1680, 1008 cm^{-1}; ESIMS *m/z* 351 $[M+Na]^+$; HRESIMS *m/z* 329.1744 $[M+H]^+$ (calcd for $C_{20}H_{25}O_4$ $[M+H]^+$, 329.1752); For ^1H and ^{13}C NMR spectroscopic data, see Tables 2 and 3.

4.3.13. Crystallographic data for compound **2**

$C_{20}H_{24}O_3$, M = 312.39, colorless needles (MeOH), space group $P2_1$, α = 6.2583(10) Å, *b* = 8.1583(13) Å, *c* = 17.088(3) Å, $\alpha = \gamma = 90°$, β = 94.533(2)°, *V* = 869.8(2) $Å^3$, *Z* = 2, *d* = 1.193 g/cm^3, crystal dimensions 0.12 × 0.22 × 0.77 mm was used for measurements on a Bruker APEX DUO diffractometer with a graphite monochromator (Φ/ω scans), Mu K_α radiation. The total number of independent reflections measured was 4664, of which 4242 were observed ($|F|^2 \geqslant 2\sigma|F|^2$). Final indices: R_1 = 0.0360, wR_2 = 0.0888 ($w = 1/\sigma|F|^2$), *S* = 1.065, Flack coefficient 0.5(8). The crystal structure of **2** was solved by direct method SHELXS-97 (Sheldrich, G.M. University of Gottingen: Gottingen, Germany, 1997) and the full-matrix least-squares calculations. Crystallographic data for the structure of **2** have been deposited in the Cambridge Crystallographic Data Centre (deposition number: CCDC 850175). Copies of these data can be obtained free of charge via the Internet at www.ccdc.cam.ac.uk/conts/retrieving.html (or from the Cambridge Crystallographic Data Centre, 12 Union Road, Cambridge CB21EZ, U.K.; fax: (+44) 1223-336-033; or deposit@ccdc.cam.ac.uk).

4.4. Cytotoxicity assay

Colorimetric assays were performed to evaluate each compound's activity. A panel of human tumor cell lines was used: breast cancer MCF-7, hepatocellular carcinoma SMMC-7721, human myeloid leukemia HL-60, colon cancer SW480 and lung cancer A-549. The cell lines were provided by Shanghai cell bank in China. All the cells were cultured in RPMI-1640 or DMEM medium (Hyclone, USA), supplemented with 10% fetal bovine serum (Hyclone, USA) at 37 °C in a humidified atmosphere with 5% CO_2.

The cytotoxicity assay was conducted according to the MTT (2-(4,5-dimethylthiazol-2-yl)-2,5-diphenyltetrazolium bromide) method in 96-well microplates (Mosmann, 1983). After compound treatment, cell viability was detected at 595 nm in a 96-well microtiter plate reader (Bio-Rad 680) and a cell growth curve was graphed. The IC_{50} value of each compound was calculated by Reed and Muench's method (Reed and Muench, 1938). The experiments were performed at least three times, with each experiment consisting of samples in triplicate.

Acknowledgments

The authors are grateful to Professor Chengyuan Yang of the Xishuangbanna Tropical Botanical Garden, Chinese Academy of Sciences, for identification of the plant. This work was supported financially by Key Program of National Key Technology Support Program (No.2007BAD32B01-03) and Special foundation of National Major Basic Research Program (SB2007FY400) of National Ministry of Science and Technology of China, the National Natural Science Foundation of China (No. 81202437), the National Knowledge Innovation Program of Chinese Academy of Sciences (Grant Nos. KSCX2-YW-G-038).

Appendix A. Supplementary data

Supplementary data associated with this article can be found, in the online version, at http://dx.doi.org/10.1016/j.phytochem.2013.09.008.

References

Achten, W.M.J., Nielsen, L.R., Aerts, R., Lengkeek, A.G., Kjær, E.D., Trabucco, A., Hansen, J.K., Maes, W.H., Graudal, L., Akinnifesi, F.K., Muys, B., 2010. Towards domestication of *Jatropha curcas*: a review. Biofuels 1, 91–107.

Aiyelaagbe, O.O., Hamid, A.A., Fattorusso, E., Taglialatela-Scafati, O., Schroder, H.C., Muller, W.E.G., 2011. Cytotoxic activity of crude extracts as well as of pure components from *Jatropha* species, plants used extensively in African Traditional Medicine. Evid-Based Compl. Alt. 2011. Article ID 134954, 7 pages. http://dx.doi.org/10.1155/2011/134954.

Burkill, H.M., 1994. The Useful Plants of West Tropical Africa. Royal Botanical Gardens, Kew, UK.

Can-Ake, R., Erosa-Rejon, G., May-Pat, F., Pena-Rodriguez, L.M., Peraza-Sanchez, S.R., 2004. Bioactive terpenoids from roots and leaves of *Jatropha gaumeri*. Rev. Soc. Quim. Mex. 48, 11–14.

Chianese, G., Fattorusso, E., Aiyelaagbe, O.O., Luciano, P., Schroder, H.C., Muller, W.E.G., Taglialatela-Scafati, O., 2011. Spirocurcasone, a diterpenoid with a novel carbon skeleton from *Jatropha curcas*. Org. Lett. 13, 316–319.

Devappa, R.K., Makkar, H.P.S., Becker, K., 2011. *Jatropha* diterpenes: a review. J. Am. Oil Chem. Soc. 88, 301–322.

Ekundayo, F.O., Adeboye, C.A., Ekundayo, E.A., 2011. Antimicrobial activities and phytochemical screening of pignut (*Jatrophas curcas* Linn.) on some pathogenic bacteria. J. Med. Plants Res. 5, 1261–1264.

Fairless, D., 2007. Biofuel: the little shrub that could-maybe. Nature 449, 652–655.

Jakupovic, J., Grenz, M., Schmeda-Hirschmann, G., 1988. Rhamnofolane derivatives from *Jatropha grossidentata*. Phytochemistry 27, 2997–2998.

Liu, J.Q., Yang, Y.F., Wang, C.F., Li, Y., Qiu, M.H., 2012. Three new diterpenes from *Jatropha curcas*. Tetrahedron 68, 972–976.

Mosmann, T., 1983. Rapid colorimetric assay for cellular growth and survival: application to proliferation and cytotoxicity assays. J. Immunol. Methods 65, 55–63.

Muangman, S., Thippornwong, M., Tohtong, R., 2005. Anti-metastatic effects of curcusone B, a diterpene from *Jatropha curcas*. In Vivo 19, 265–268.

Naengchomnong, W., Thebtaranonth, Y., Wiriyachitra, P., Okamoto, K.T., Clardy, J., 1986. Isolation and structure determination of four novel diterpenes from *Jatropha curcas*. Tetrahedron Lett. 27, 2439–2442.

Oliver-Bever, B., 1986. Medicinal Plants in Tropical West Africa. Cambridge University Press, London, UK.

Pertino, M., Schmeda-Hirschmann, G., Rodriguez, J., Theoduloz, A.C., 2007. Gastroprotective effect and cytotoxicity of semisynthetic jatropholone derivatives. Planta Med. 73, 1095–1100.

Picha, P., Naengchomnong, W., Promratanapongse, P., Kano, E., Hayashi, S., Ohtsubo, T., Zhang, S.W., Shioura, H., Kitai, R., 1996. Effect of natural pure compounds curcusones A and C from tropical herbal plant *Jatropha curcus* on thermosensitivity and development of thermotolerance in Chinese hamster V-79 cells in vitro. J. Exp. Clin. Cancer Res. 15, 177–183.

Ravindranath, N., Ramesh, C., Das, B., 2003. A rare dinorditerpene from *Jatropha curcas*. Biochem. Syst. Ecol. 31, 431–432.

Reed, L.J., Muench, H., 1938. A simple method of estimating fifty percent endpoints. Am. J. Hyg. 27, 493–497.

Sutthivaiyakit, S., Mongkolvisut, W., Prabpai, S., Kongsaeree, P., 2009. Diterpenes, sesquiterpenes, and a sesquiterpene-coumarin conjugate from *Jatropha integerrima*. J. Nat. Prod. 72, 2024–2027.

Sutthivaiyakit, S., Mongkolvisut, W., Ponsitipiboon, P., Prabpai, S., Kongsaeree, P., Ruchirawat, S., Mahidol, C., 2003. A novel 8,9-*seco*-rhamnofolane and a new rhamnofolane endoperoxide from *Jatropha integerrima* roots. Tetrahedron Lett. 44, 3637–3640.

Sahidin, Nakazibwe, S., Taher, M., Saxena, A.K., Ichwan, S.J.A., Ardiyansyah, 2011. Antiproliferative activity of curcusone B from *Jatropha curcas* on human cancer cell lines. Aust. J. Basic Appl. Sci. 5, 47–51.

Wang, X.C., Zheng, Z.P., Gan, X.W., Hu, L.H., 2009. Jatrophalactam, a novel diterpenoid lactam isolated from *Jatropha curcas*. Org. Lett. 11, 5522–5524.

Xu, J.J., Fan, J.T., Zeng, G.Z., Tan, N.H., 2011. A new tetracyclic diterpene from *Jatropha curcas*. Helv. Chim. Acta 94, 842–846.

Zhang, X.Q., Li, F., Zhao, Z.G., Liu, X.L., Tang, Y.X., Wang, M.K., 2012. Diterpenoids from the root bark of *Jatropha curcas* and their cytotoxic activities. Phytochem. Lett. 5, 721–724.